Optical and Microwave-Assisted Digital Detection of Magnetic Field with NV^- Centers in Diamond

Fabrizio Moro

Department of Materials Science, University of Milano-Bicocca, Milano 20125, Italy.

ABSTRACT

Magnetometry based on Optically Detected Magnetic Resonance (ODMR) of NV^- colour centers in diamond is a well-established method for sensitive detection of magnetic field intensity and direction. However, ODMR spectra are inherently independent of magnetic field polarity which is a key parameter for applications such as reading of magnetic bits in HDD and for the understanding of physical phenomena in nanomagnetism. Recently a method has been implemented for digital detection of magnetic field polarity by NV^- centers in diamond simply by monitoring the changes of a magnetic field demodulated photoluminescence (PL) signal in condition of magnetic resonance (*i.e*. microwave assisted or ODMR) Unlike other methods, the demodulated PL signal shows a complete sign inversion rather than an intensity shift, thus making the detection of magnetic field polarity direct and unambiguous. Here, it is reported that the same method can be applied to off-resonance condition (*i.e*. optical), that is by detecting the photoluminescence signal locked to a demodulating magnetic field without microwave resonant excitation, which simplifies the set-up. Furthermore, a sensitivity study has been conducted resulting in up-to-standard sensitivities of a few $\mu T/\sqrt{Hz}$ for both microwave-assisted and only-optical detection in a low-cost and simple cw-ODMR set-up. It is concluded that the simplified set-up required for the optical method comes at expense of reduction of sensitivity by 36%. Overall, potentially these features make the demodulated PL on magnetic resonance as well as off resonance suitable for real-time digital detection of magnetic field of magnetic bits in HDDs and for the study of magnetic phenomena at nanoscale.

INTRODUCTION

Magnetometers enable the detection of magnetic field intensity and direction, and play a crucial role in various fields from geophysics, medicine, space science to the understanding of novel magnetic phenomena at nanoscale.[1] High sensitivity to magnetic field intensity is a key parameter to extract accurate information from the system under study. The most sensitive magnetometers include fluxgate magnetometers, proton precession magnetometers, optically pumped magnetometers, superconducting quantum interference devices (SQUIDs). More recently, negatively charged nitrogen-vacancy (NV^-) colour centers in diamond[2] have demonstrated high sensitivity to nanoscale magnetic field detection under ambient conditions; thus opening new frontiers in biological imaging,[3] material science,[4, 5] and quantum sensing.[6] Magnetometers base on NV^- centers in diamond relies on a Optically Detected Magnetic Resonance (ODMR)[7, 8] which detects magnetic resonance transitions via changes of the photoluminescence (PL) signal. ODMR enables direct measurements of magnetic field vector direction and magnitude by observing the Zeeman separation of the ODMR signals of the four magnetically inequivalent NV^- spin centers ($S = 1$) in the diamond crystal structure. In some applications the magnetic field polarity is of interest such as read-out of digital information in magnetic Hard Disk Devices (HDD)[9] as well as for the detection of magnetic orders and phenomena in nanomagnetism such as magnetic vortexes.[5] In this regard, ODMR spectra are inherently insensitive to magnetic field polarity.[10] This limitation can be overcome with the application of a bias magnetic field,[5, 11] or by using circularly polarized microwave excitations (σ^+ or σ^-).[12-14] In the first case a bias magnetic field is used to separate the eight ODMR dips corresponding to four doublets resonances of the NV^- sites. The PL signal of the ODMR dips due to the sample's stray field is monitored at maximum slope. A shift of the ODMR resonance dips to higher or lower frequency occurs depending on the sample magnetic field polarity, thus resulting in an increase or decrease of the PL signal, respectively. The second method relies on the selectivity of the electron spin transitions $m_s = 0 \rightarrow +1$ and $0 \rightarrow -1$ by left (σ^-) and

right (σ^+) circular microwave polarization respectively. Thus, for a given polarization only one of the two electron spin transitions is observed depending of the magnetic field polarity. More, recently a new method has been proposed where the symmetry of the first-derivative ODMR spectral lines recorded after demodulation of a small applied magnetic field directly correlates to the magnetic field polarity.[15] This method opens up unambiguous and direct real time detection of the magnetic field polarity. Here, it is found that the "demodulation field" method can be implemented off-resonance condition (*i.e.* optical) that is by detecting the photoluminescence signal locked to a demodulating magnetic field. Unlike ODMR (*i.e.* microwave-assisted) where a microwave source in proximity of the diamond is required to match the magnetic resonance condition, the optical method (*i.e.* microwave-free) provides a simpler set-up with a more straightforward implementation in microscopy application.[9] More importantly, the optical method avoids heating effects due to high power microwaves, thus enabling magnetometry studies of sensitive samples such as high transition-temperature superconductors, two-dimensional magnetic materials, and biological samples.[9, 16-19]

Furthermore, the sensitivity of the optical and microwave-assisted methods have been investigated with the aim to extract the smallest magnetic field intensity and polarity. The two methods are compared to find out their potentialities and limitations in view of their applications in magnetometry.

The article is organized as follows: preliminary studies have been conducted to extract the optimal modulation amplitude and frequency for the highest sensitivity measurement. Then, an experiment has been realized to explore the potential of optical and microwave-assisted digital detection of a magnetic field whose polarity is switched from positive to negative alternatively, thus simulating digital detection encoded in magnetic bits of magnetic HDDs or magnetization dynamics of a magnetic sample. Finally, the results are compared with other methods previously reported in literature.

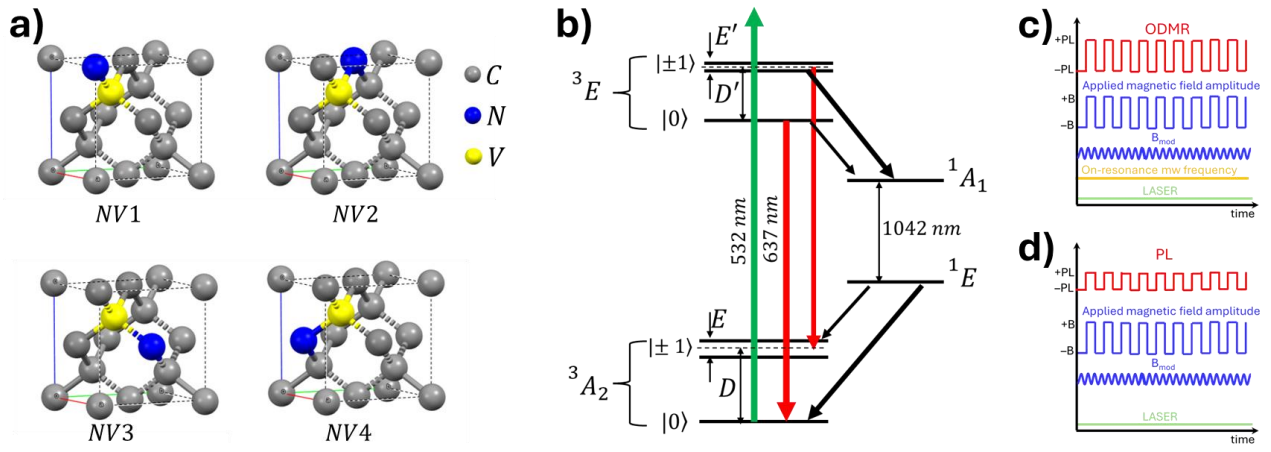

Figure 1 a) Crystal structure of diamond with NV^- centers in the four inequivalent positions (NV1, NV2, NV3 and NV4) within the unit cell. Red, green and blue axes correspond to the *a*, *b* and *c* crystallographic axes respectively. **b)** Jablonski energy level diagram (not in scale) of a NV^- center ($S = 1$) with axial and rhombic zero field splitting for the ground state, *D* and *E* and the excited state, *D'* and *E'*. Arrows thickness indicates transition probabilities. Schemes of the magnetic field modulated photoluminescence signal in condition of magnetic resonance (*i.e.* microwave assisted or ODMR) (**c**) and off-resonance (*i.e.* optical), (**d**).

RESULTS AND DISCUSSION

Figure 1a shows the diamond structure within the unit cell with the NV^- center and its C_{3v} symmetry. The nitrogen atom can replace any of the four carbon sites in the diamond tetrahedron, thus providing four inequivalent NV^- centers each with its own spin quantization axis. In **Figure 1b** is reported the Jablonski diagram with the $S = 1$ ground and excited states zero-field split by axial (*D*) and rhombic (*E*) distortions. In zero magnetic field the four NV^- sites are magnetically equivalent. When an external magnetic field is applied the energy levels are split by Zeeman interaction, and each NV^- site experiences a different magnetic field projection, thus resulting in

four doublets in the ODMR spectrum.

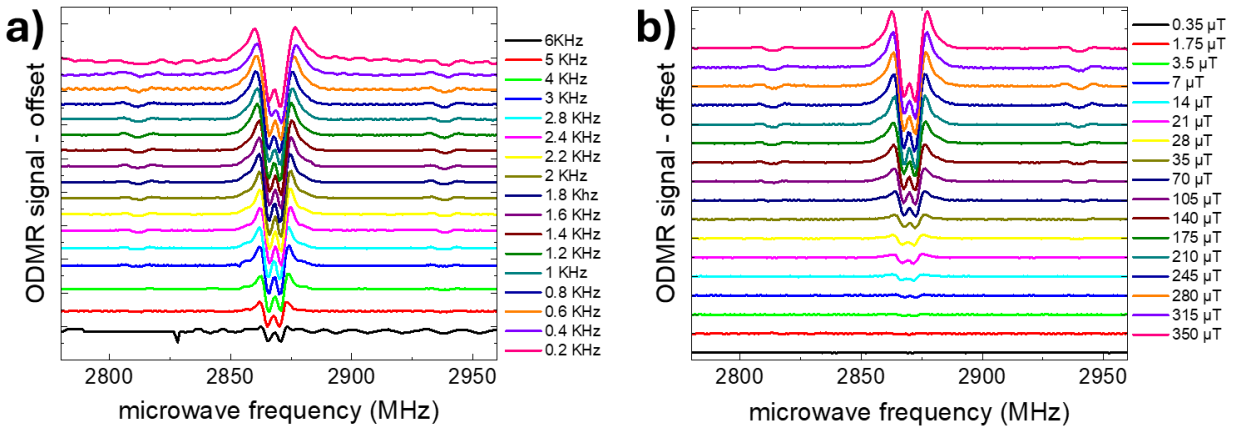

Figure 2. ODMR spectra recorded at fixed modulation amplitude B_{mod} = 350 µT and different frequencies (**a**) and at fixed 1.6 KHz modulation frequency and different B_{mod} (**b**).

Figure 2 shows the ODMR spectra recorded on NV^- centers in diamond by demodulating an oscillating magnetic field (B_{mod}), (**Figure 1c**). In order to find the optimal signal-to-noise ratio (S/N, the ODMR spectra are recorded as function of the magnetic field frequency at the maximum B_{mod} amplitude. From these spectra the peak-to-peak intensities (I_{pp}) and linewidths (LW_{pp}) have been

extracted and plotted as function of the frequency in **Figure 3**.

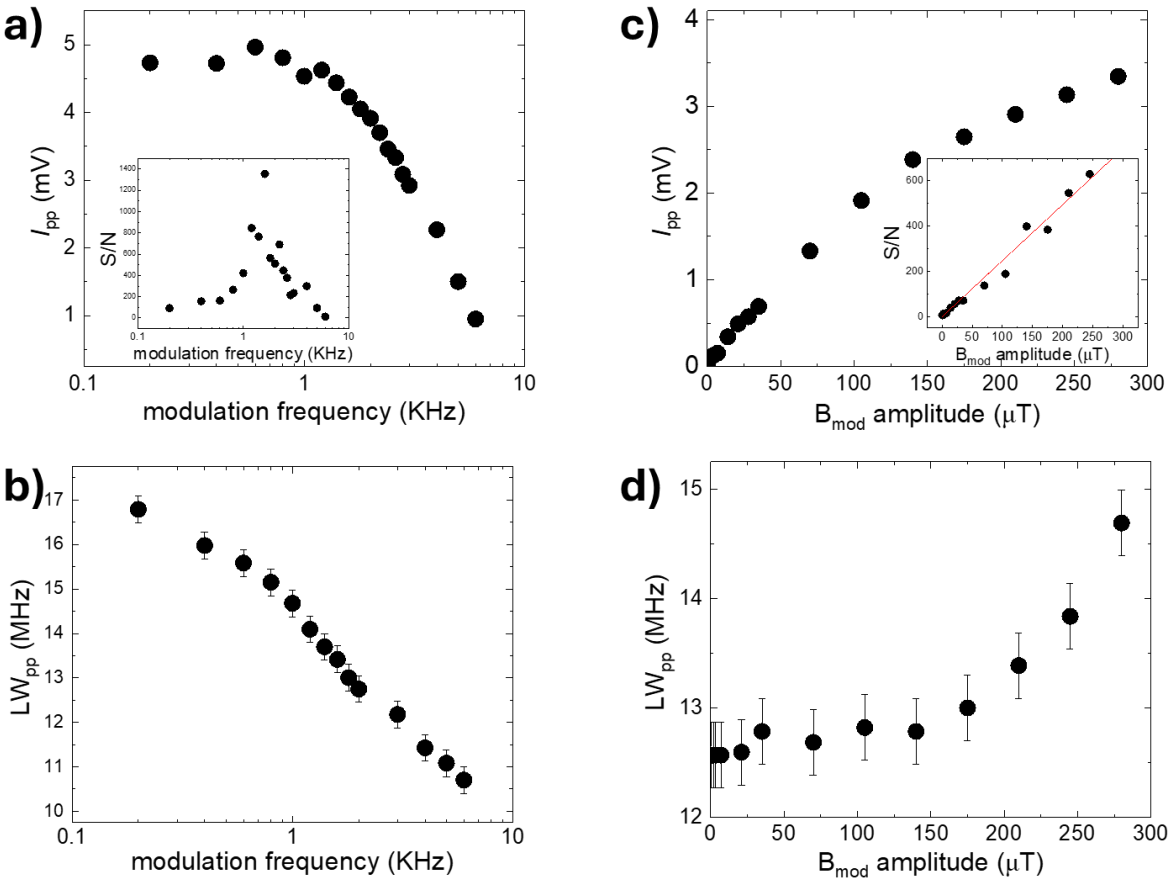

Figure 3 Peak-to-peak intensity (I_{pp}) versus modulation field frequency (**a**) and amplitude (**b**) and peak-to-peak linewidth (LW_{pp}) as function of the modulation field frequency (**c**) and B_{mod} amplitude (**d**). Insets in (**a**) and (**b**) are the signal to noise ratios of the data reported in the main graphs.

The semi-log plot I_{pp} as function of the microwave frequency shows a constant value in the range 0.1 – 1 KHz with a steep decrease for higher frequencies (**Figure 3a**). A low-pass filter has been applied after signal demodulation and it is adjusted to reach low noise signal without cutting the frequency signals near DC. The S/N obtained by dividing the I_{pp} by the standard deviation (SD) of the off-resonance spectral range shows a maximum at (1.6 ± 0.2) KHz with a low-pass filter of 5 Hz. Instead, LW_{pp} shows a monotonic decrease with frequency **Figure 3b**. Therefore, a modulation frequency of 1.6 KHz has been chosen as the "best" frequency. The next step is to search for

optimal magnetic field modulation amplitude. The results reported in **Figure 3c** show that the I_{pp} increases linearly for $B_{mod} < 100$ μT, and for larger values it increases monotonically without reaching saturation. The S/N ratio (inset of **Figure 3c**) increases linearly across the whole magnetic field modulation amplitude. The spectral linewidth is constant for $B_{mod} < 150$ μT, and it increases for larger values (**Figure 3d**). The effect of the magnetic field modulation amplitude translates into modulation of the microwave amplitude due the Zeeman effect, which in turn translates into a modulation of the PL signal. A larger modulation amplitude implies a modulation of larger portion of the photoluminescence spectrum which leads to a larger PL signal. However, when the modulation amplitude becomes comparable to about a third of the narrowest spectral line the spectrum becomes distorted, the photoluminescence decreases, and the spectral resolution is reduced. From these data the optimal combination of modulation frequency and magnetic field amplitude for largest S/N ratio of ODMR spectra is 1.6 KHz and $B_{mod} = 150$ μT. For highly-sensitive detection of the magnetic field of soft magnets and antiferromagnets it is crucial that the B_{mod} does not perturb their intrinsic magnetic properties. Therefore, the smallest modulation amplitude is desirable. From the fitting of the S/N versus B_{mod} it is extracted a magnetic field of ~ 0.4 μT for a S/N ratio of ~ 1 (inset **Figure 3c**). This value sets the lower bound for magnetic field amplitude necessary to detect a signal. In practice, a value larger than two or three times is necessary.

Finally, an experiment has been realized to test the capability to detect the polarity of a magnetic field whose sign is alternatively changed from positive to negative. Two methods are compared: optical and microwave-assisted lock-in detection both with the aid of demodulating magnetic field (**Figure 1c** and **1d**). The two methods can be implemented on the same ODMR experiment with the only difference that while detecting the PL signal the microwaves are turned on-resonance or off-resonance. A primary and a secondary coils are used to generate the fast oscillating magnetic field (~ KHz), and the low frequency (~ Hz) square-wave magnetic field directed along one direction (+)

and its opposite (–). The secondary coil simulates a sample's stray field. The amplitude of the magnetic fields of both coils at the diamond position are calibrated with an Hall probe. The ODMR spectra are firstly recorded consecutively by setting the secondary coil to + and – magnetic field polarities (**Figure 4a**). The ODMR spectra show three man features: (i) the background off-set level shifts from positive to negative values (ΔPL), (ii) the ODMR resonances occurring as first-derivative lineshape have opposite symmetries (ΔODMR), (iii) for each spectrum the symmetries of first-derivative lineshapes are opposite for the m_s: 0 → +1 and 0 → –1 transitions. The observations (ii) and (iii) have been previously analyzed and a *proof-of-concept* experiment has been carried out to demonstrate digital detection with ODMR.[15] Instead point (i) is shown for the first time to enable digital detection of magnetic fields with relatively high sensitivity. In addition, a direct comparison between the optical and ODMR is provided to find out which method is more sensitive to magnetic field amplitude and polarity.

It is first noted that the ΔPL shifts from positive to negative values in **Figure 4a** occurs as result of the spin-mixing of the m_s states with the application of a magnetic field orientated off to the NV spin quantization axis.[20] By applying the square-like varying magnetic field, the average lifetime of the m_s states for the ensemble of NV^- centers is changed, depending on the magnitude and polarity of the magnetic field.

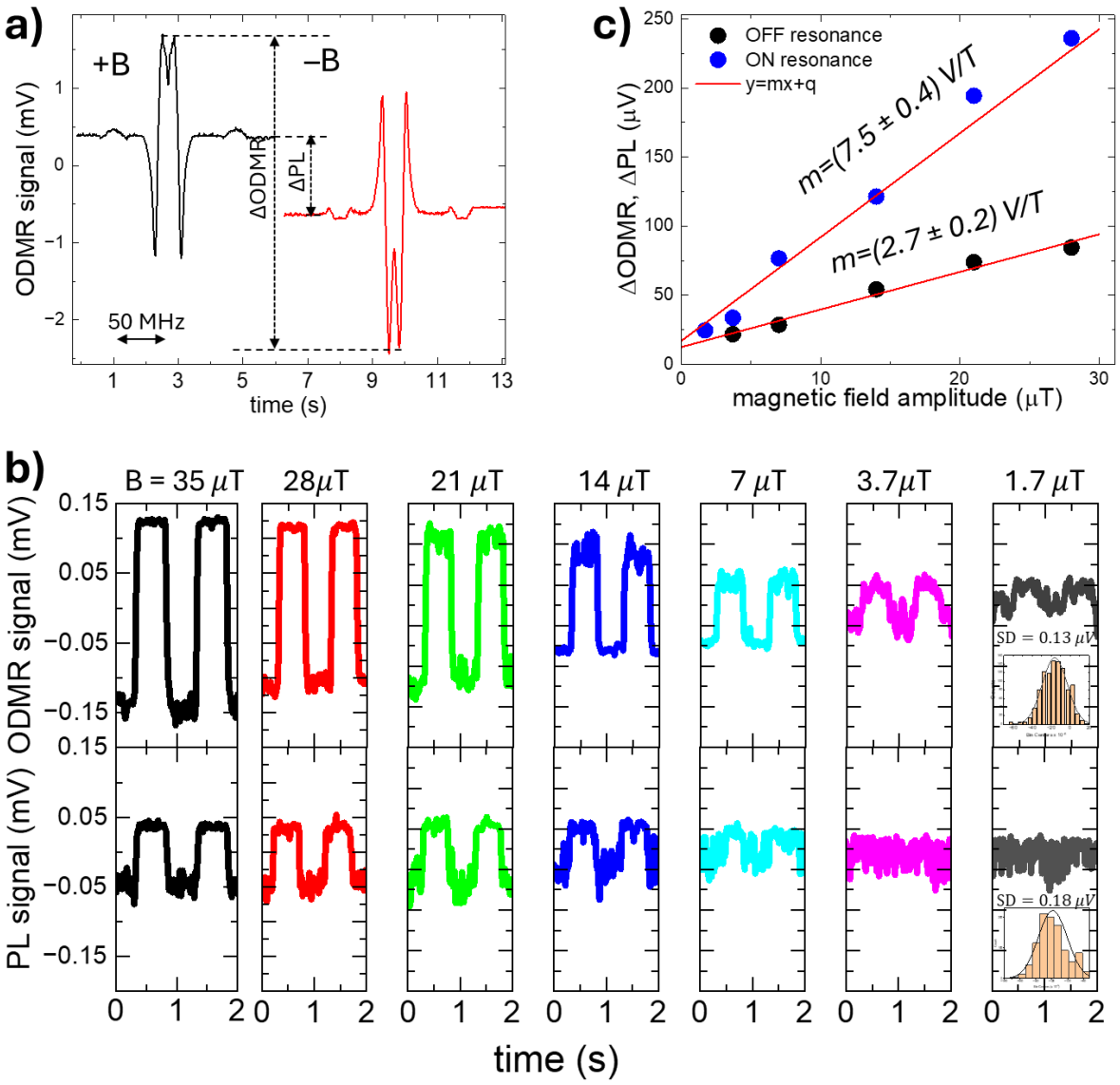

Figure 4 a) ODMR spectra recorded consecutively for opposite polarities of an applied magnetic field. The change of the ODMR and PL intensities are indicated with ΔODMR and ΔPL. **b**) Real-time detection of the ODMR (on-resonance, *i.e.* ν = 2870.5 MHz) and PL (off-resonance) changes due to an 1 Hz square-wave magnetic field with different amplitudes. Insets: Gaussian statistical distributions of the data with standard deviations. **c**) on-resonance and off-resonance, ΔODMR and ΔPL signals extracted from (**b**) and plotted as function of the magnetic field amplitude.

The results reported in **Figure 4b** show the magnetic field demodulated PL signal for different strengths of B_{mod} oscillating at 1 Hz with microwaves set to on-resonance (*i.e.* ν = 2870.5 MHz) and off-resonance In both cases, the demodulated PL signal alternates symmetrically from positive to

negative values, thus demonstrating the potential to effectively probe a digital magnetic field information encoded in the polarity. Finally, the sensitivity of the two methods has been analyzed by reporting the ΔPL and ΔODMR signals extracted from **Figure 4b** as function of B_{mod}. The slope of the linear fit of the curves provides direct estimation of the sensitivities: (7.5 ± 0.4) V/T and (2.7 ± 0.2) V/T for on and off-resonance respectively (**Figure 4c**). The microwave-assisted method gives a sensitivity larger than the optical method by ~ 36 %.

The lowest magnetic field detectable has been estimated by calculating the standard deviation (SD) of the noise level and dividing it by the sensitivity and the low-pass filter of 5 Hz used for lock-in detection. The results for the SDs are: 13 μV and 18 μV for on and off resonance respectively, and the corresponding sensitivities are: (0.8 ± 0.1) $\mu T/\sqrt{Hz}$ and (2.9 ± 0.5) $\mu T/\sqrt{Hz}$.

Currently, the best magnetic field sensitivity achieved with NV^- centers by using pulsed-ODMR protocols (*e.g.* Han echo) is of the order of 1 nT/√Hz for a single NV^- center in a single crystal diamond. Higher sensitivity can be achieved in an NV^- ensemble leading to a pT/√Hz sensitivity.[4, 21] The results reports in this work are in line and potentially better than continuous wave (cw) ODMR studies on single or ensemble NV^- centers at room temperature ~ 1-10 μT/√Hz.[6, 22, 23] These sensitivities will potentially enable the detection of the magnetic moment of a single electron spin up at 10 nm distance. These finding suggests that it is possible to detect the magnetic field induced by a range of nanomaterials including biological molecules (*e.g.* ferritine),[24, 25] molecular magnets,[26] organic molecules (*e.g.* pentacene),[27, 28] magnetic nanoparticles (*e.g.* iron oxide),[29] skyrmions,[11] spin-defects in semiconductors,[30-32] magnetism of thin films and 2D magnets.[31, 33] Considering the low cost set-up and simple cw-ODMR method used in this work, the sensitivity can be easily competitive with the high sensitivity achieved with pulsed-ODMR methods. Furthermore, this method offers some advantages compared to the other methods, *i.e.* magnetic bias field[5, 11] and microwave circular polarization.[12-14] In fact the methods described in this work makes use of a small μT magnetic field oscillating at a few KHz instead of the mT magnetic field required for the

"bias field" method. Thus, the stray magnetic field from antiferromagnets and fragile spin configurations in magnetic vortexes in nanomagnetism could be detected with minimal perturbation of the intrinsic magnetization. In addition, this method requires a simple microstripline carrying linearly polarized microwaves instead of more complicated stripline designs where high degree control of the microwave polarization is required.

CONCLUSION

A method has been implemented for digital detection of magnetic field by NV^- colour centers in diamond. A demodulated photoluminescence signal by an oscillating small magnetic field has been monitored while applying a square wave magnetic field amplitude. The experiment has been conducted with two approaches: only optical detection (i.e. microwave free) as well as assisted by on resonance microwave excitation. The results indicate that the optical signal switches sign upon inversion of the magnetic field polarity. A relatively high sensitivity of $(0.8 \pm 0.1)\ \mu T/\sqrt{Hz}$ and $(2.9 \pm 0.5)\ \mu T/\sqrt{Hz}$ has been reported for microwave-assisted and optical detection respectively with a low-cost set-up and simple cw-ODMR. This method is particularly convenient for applications where the magnetic field polarity is of interest such as magnetic bits in HDDs and magnetic phenomena at nanoscale. Unlike other methods based on millitesla bias magnetic field or microwave circular polarizations, here a microtesla magnetic field is employed. Finally, it is concluded that the microwave-free method provides a simpler implementation compared to the microwave assisted-method at the expense of the reduction of the sensitivity by 36%. In addition, it avoids heating and interference effects due to high power microwaves, thus making the method suitable for the study of sensitive samples such antiferromagnets and soft ferromagnets, high transition-temperature (Tc) superconductors and biological samples.

MATERIALS AND METHODS

Materials: 150 micron Red Fluorescent Microdiamond with concentration of NV^- ~ 2.5-3 ppm were purchased from Adámas NanoTechnologies Inc. A single crystal was glued on a microstripline.

Optical set-up: A diode pumped solid state (DPSS) laser (Thorlabs DJ532-40) mounted on a current and temperature controller (Thorlabs LDM56F and LDC200C) was used as optical excitation source. The laser beam was directed with a dichroic mirror to a 10x objective with nominal aperture 0.25. The photoluminescence was detected with a silicon photodiode, 350 - 1100 nm, (Thorlabs, SM1PD1B), amplified with a transimpedance photocurrent amplifier (Thorlabs PDA200C) and sent to a MOKU:GO (Liquid Instruments) reconfigurable FPGA oscilloscope/lock-in amplifier interfaced with a PC.

Microwave module: a microwave module was assembled with a ADF4351 generator (35 – 4400 MHz) controlled by microprocessor for adjustable frequency sweeps.[34] The microwave signal was 40 dB broadband amplified (max output power 100 mW) for strong excitation and maximization of the ODMR contrast before feeding a broad band microstripline realized on a single face copper board and FR4 dielectric with thicknesses of 35 μm and 1.6 mm, respectively and terminated with 50 Ω load.

Magnets. Home-made coils with N = 1000 turns and diameter 3 cm.

Data acquisition: The photoluminescence was detected on channel 1 of the oscilloscope as function of time while sweeping the microwave frequency whose start and stop frequency sweep logic-input is fed into channel 2. The ODMR spectrum is built up by time to frequency conversion. Lock-in detection was made with time constant 20 ms (12 dB/octave) and variable modulation frequency and amplitude. All measurements were conducted at room temperature.

DATA AVAILABLITY

Data will be made available on request.

DECLARATION OF COMPETING INTEREST

The authors declare that they have no known competing financial interests or personal relationships that could have appeared to influence the work reported in this paper.

ACKNOWLEDGEMENTS

F.M. gratefully acknowledge financial support by Rete Interdipartimentale di Spettroscopia (project BIR2021) through the “fondi per le grandi attrezzature” University of Milano-Bicocca and PNRR MUR project (PE0000023-NQSTI).

REFERENCES

(1) Grosz, A.; Haji-Sheikh, M. J.; Mukhopadhyay, S. C. *High Sensitivity Magnetometers*; Smart sensors, measurement and instrumentation; 19; Springer International Publishing : Imprint : Springer, 2017. DOI: 10.1007/978-3-319-34070-8.
(2) Doherty, M. W.; Manson, N. B.; Delaney, P.; Jelezko, F.; Wrachtrup, J.; Hollenberg, L. C. L. The nitrogen-vacancy colour centre in diamond. *Phys. Rep. Rev. Sec. Phys. Lett.* **2013**, *528* (1), 1-45, DOI: 10.1016/j.physrep.2013.02.001.
(3) Schirhagl, R.; Chang, K.; Loretz, M.; Degen, C. L. Nitrogen-Vacancy Centers in Diamond: Nanoscale Sensors for Physics and Biology. *Annu. Rev. Phys. Chem.* **2014**, *65*, 83-105, DOI: 10.1146/annurev-physchem-040513-103659.
(4) Boretti, A.; Rosa, L.; Blackledge, J.; Castelletto, S. Nitrogen-vacancy centers in diamond for nanoscale magnetic resonance imaging applications. *Beilstein J. Nanotechnol.* **2019**, *10*, 2128-2151, DOI: 10.3762/bjnano.10.207.

(5) Rondin, L.; Tetienne, J. P.; Hingant, T.; Roch, J. F.; Maletinsky, P.; Jacques, V. Magnetometry with nitrogen-vacancy defects in diamond. *Rep. Prog. Phys.* **2014**, *77* (5), DOI: 10.1088/0034-4885/77/5/056503.
(6) Barry, J. F.; Schloss, J. M.; Bauch, E.; Turner, M. J.; Hart, C. A.; Pham, L. M.; Walsworth, R. L. Sensitivity optimization for NV-diamond magnetometry. *Rev. Mod. Phys.* **2020**, *92* (1), DOI: 10.1103/RevModPhys.92.015004.
(7) Yavkin, B. V.; Soltamov, V. A.; Babunts, R. A.; Anisimov, A. N.; Baranov, P. G.; Shakhov, F. M.; Kidalov, S. V.; Vul, A. Y.; Mamin, G. V.; Orlinskii, S. B. Defects in Nanodiamonds: Application of High-Frequency cw and Pulse EPR, ODMR. *Appl. Magn. Reson.* **2014**, *45* (10), 1035-1049, DOI: 10.1007/s00723-014-0582-y.
(8) Cavenett, B. C. Optically detected magnetic resonance (ODMR) investigation of recombination processes in semiconductors. *Adv. Phys.* **1981**, *30* (4), 475-538, DOI: 10.1080/00018738100101397.
(9) Rondin, L.; Tetienne, J. P.; Spinicelli, P.; Dal Savio, C.; Karrai, K.; Dantelle, G.; Thiaville, A.; Rohart, S.; Roch, J. F.; Jacques, V. Nanoscale magnetic field mapping with a single spin scanning probe magnetometer. *Appl. Phys. Lett.* **2012**, *100* (15), DOI: 10.1063/1.3703128.
(10) Harrison, J.; Sellars, M. J.; Manson, N. B. Optical spin polarisation of the N-V centre in diamond. *J. Lumin.* **2004**, *107* (1), 245-248, DOI: https://doi.org/10.1016/j.jlumin.2003.12.020.
(11) Rondin, L.; Tetienne, J. P.; Rohart, S.; Thiaville, A.; Hingant, T.; Spinicelli, P.; Roch, J. F.; Jacques, V. Stray-field imaging of magnetic vortices with a single diamond spin. *Nat. Commun.* **2013**, *4* (1), 2279, DOI: 10.1038/ncomms3279.
(12) Alegre, T. P. M.; Santori, C.; Medeiros-Ribeiro, G.; Beausoleil, R. G. Polarization-selective excitation of nitrogen vacancy centers in diamond. *Phys. Rev. B* **2007**, *76* (16), DOI: 10.1103/PhysRevB.76.165205.
(13) Herrmann, J.; Appleton, M. A.; Sasaki, K.; Monnai, Y.; Teraji, T.; Itoh, K. M.; Abe, E. Polarization- and frequency-tunable microwave circuit for selective excitation of nitrogen-vacancy spins in diamond. *Appl. Phys. Lett.* **2016**, *109* (18), DOI: 10.1063/1.4967378.
(14) Pribosek, J.; Eder, M.; Caponi, D.; Mullen, C. Quantum diamond microscope with circularly polarized microwave excitation for wide-field vector magnetometry. In *Conference on Quantum Technologies*, Strasbourg, FRANCE, Apr 08-10, 2024; 2024; Vol. 12993. DOI: 10.1117/12.3029598.
(15) Moro, F. Detection of magnetic field polarity with magnetic field modulation ODMR on NV– centers in diamond. *Applied Materials Today* **2025**, *44*, 102762, DOI: https://doi.org/10.1016/j.apmt.2025.102762.

(16) Thiel, L.; Wang, Z.; Tschudin, M. A.; Rohner, D.; Gutiérrez-Lezama, I.; Ubrig, N.; Gibertini, M.; Giannini, E.; Morpurgo, A. F.; Maletinsky, P. Probing magnetism in 2D materials at the nanoscale with single-spin microscopy. *Science* **2019**, *364* (6444), 973-+, DOI: 10.1126/science.aav6926.
(17) Bürgler, B.; Sjolander, T. F.; Brinza, O.; Tallaire, A.; Achard, J.; Maletinsky, P. All-optical nuclear quantum sensing using nitrogen-vacancy centers in diamond. *Npj Quantum Inform.* **2023**, *9* (1), DOI: 10.1038/s41534-023-00724-6.
(18) Wickenbrock, A.; Zheng, H. J.; Bougas, L.; Leefer, N.; Afach, S.; Jarmola, A.; Acosta, V. M.; Budker, D. Microwave-free magnetometry with nitrogen-vacancy centers in diamond. *Appl. Phys. Lett.* **2016**, *109* (5), DOI: 10.1063/1.4960171.
(19) Akhmedzhanov, R.; Gushchin, L.; Nizov, N.; Nizov, V.; Sobgayda, D.; Zelensky, I.; Hemmer, P. Microwave-free magnetometry based on cross-relaxation resonances in diamond nitrogen-vacancy centers. *Phys. Rev. A* **2017**, *96* (1), 013806, DOI: 10.1103/PhysRevA.96.013806.
(20) Lai, N. D.; Zheng, D. W.; Jelezko, F.; Treussart, F.; Roch, J. F. Influence of a static magnetic field on the photoluminescence of an ensemble of nitrogen-vacancy color centers in a diamond single-crystal. *Appl. Phys. Lett.* **2009**, *95* (13), DOI: 10.1063/1.3238467.
(21) Curilef, S. *Magnetometers - Fundamentals and Applications of Magnetism*; 2020. DOI: 10.5772/intechopen.75335.
(22) Grinolds, M. S.; Hong, S.; Maletinsky, P.; Luan, L.; Lukin, M. D.; Walsworth, R. L.; Yacoby, A. Nanoscale magnetic imaging of a single electron spin under ambient conditions. *Nat. Phys.* **2013**, *9* (4), 215-219, DOI: 10.1038/nphys2543.
(23) Taylor, J. M.; Cappellaro, P.; Childress, L.; Jiang, L.; Budker, D.; Hemmer, P. R.; Yacoby, A.; Walsworth, R.; Lukin, M. D. High-sensitivity diamond magnetometer with nanoscale resolution. *Nat. Phys.* **2008**, *4* (10), 810-816, DOI: 10.1038/nphys1075.
(24) Fescenko, I.; Laraoui, A.; Smits, J.; Mosavian, N.; Kehayias, P.; Seto, J.; Bougas, L.; Jarmola, A.; Acosta, V. M. Diamond Magnetic Microscopy of Malarial Hemozoin Nanocrystals. *Phys. Rev. Appl.* **2019**, *11* (3), DOI: 10.1103/PhysRevApplied.11.034029.
(25) Lamichhane, S.; Guevara, E. C.; Fescenko, I.; Liou, S. H.; Lai, R. Y.; Laraoui, A. Magnetic relaxometry of methemoglobin by widefield nitrogen-vacancy microscopy. *Appl. Phys. Lett.* **2024**, *125* (11), DOI: 10.1063/5.0217987.
(26) Caneschi, A.; Gatteschi, D.; Sessoli, R.; Barra, A. L.; Brunel, L. C.; Guillot, M. Alternating current susceptibility, high field magnetization, and millimeter band EPR evidence for a ground S= 10 state in [Mn12O12 (Ch3COO) 16 (H2O) 4]. 2CH3COOH. 4H2O. *J. Am. Chem. Soc.* **1991**, *113* (15), 5873-5874.

(27) Wrachtrup, J.; Vonborczyskowski, C.; Bernard, J.; Orrit, M.; Brown, R. Optically detected spin coherence of single molecues *Phys. Rev. Lett.* **1993**, *71* (21), 3565-3568, DOI: 10.1103/PhysRevLett.71.3565.
(28) Moro, F.; Moret, M.; Ghirri, A.; del Aguila, A. G.; Kubozono, Y.; Beverina, L.; Cassinese, A. Room-temperature optically detected magnetic resonance of triplet excitons in a pentacene-doped picene single crystal. *J. Mater. Res.* **2022**, *37* (6), 1269-1279, DOI: 10.1557/s43578-022-00536-y.
(29) Richards, B. A.; Ristoff, N.; Smits, J.; Perez, A. J.; Fescenko, I.; Aiello, M. D.; Hubert, F.; Silani, Y.; Mosavian, N.; Ziabari, M. S.; et al. Time-Resolved Diamond Magnetic Microscopy of Superparamagnetic Iron-Oxide Nanoparticles. *Acs Nano* **2025**, *19* (10), 10048-10058, DOI: 10.1021/acsnano.4c16703.
(30) Luo, J. L.; Geng, Y. F.; Rana, F.; Fuchs, G. D. Room temperature optically detected magnetic resonance of single spins in GaN. *Nat. Mater.* **2024**, *23* (4), DOI: 10.1038/s41563-024-01803-5.
(31) Gottscholl, A.; Kianinia, M.; Soltamov, V.; Orlinskii, S.; Mamin, G.; Bradac, C.; Kasper, C.; Krambrock, K.; Sperlich, A.; Toth, M.; et al. Initialization and read-out of intrinsic spin defects in a van der Waals crystal at room temperature. *Nat. Mater.* **2020**, *19* (5), 540-+, DOI: 10.1038/s41563-020-0619-6.
(32) Stern, H. L.; Gu, Q. S.; Jarman, J.; Barker, S. E.; Mendelson, N.; Chugh, D.; Schott, S.; Tan, H. H.; Sirringhaus, H.; Aharonovich, I.; et al. Room-temperature optically detected magnetic resonance of single defects in hexagonal boron nitride. *Nat. Commun.* **2022**, *13* (1), DOI: 10.1038/s41467-022-28169-z.
(33) Erickson, A.; Shah, S. Q. A.; Mahmood, A.; Buragohain, P.; Fescenko, I.; Gruverman, A.; Binek, C.; Laraoui, A. Imaging Local Effects of Voltage and Boron Doping on Spin Reversal in Antiferromagnetic Magnetoelectric Cr2O3 Thin Films and Devices. *Adv. Funct. Mater.* **2024**, *34* (48), DOI: 10.1002/adfm.202408542.
(34) Stegemann, J.; Peters, M.; Horsthemke, L.; Langels, N.; Glösekötter, P.; Heusler, S.; Gregor, M. Modular low-cost 3D printed setup for experiments with NV centers in diamond. *Eur. J. Phys.* **2023**, *44* (3), DOI: 10.1088/1361-6404/acbe7c.